Improved energy resolution of x-ray single photon imaging spectrometers using superconducting tunnel junctions

L. Li, L. Frunzio, C. Wilson, and D. E. Prober[a)]
Departments of Applied Physics and Physics, Yale University, Connecticut 06520-8284

A. E. Szymkowiak and S. H. Moseley
NASA Goddard Space Flight Center, Maryland 20771

(Received 14 February 2001; accepted for publication 11 June 2001)

We present measurements of the energy resolution of improved single-photon imaging x-ray spectrometers based on superconducting tunnel junctions. The devices have a Ta film absorber with an $Al/AlO_x/Al$ tunnel junction on each end. Recent device designs optimized for better quasiparticle cooling in the Al trap obtain an energy resolution of 13 eV full width at half maximum for a photon energy $E=5.9$ keV, an improvement of a factor of two over earlier devices. We also determined that the niobium contact used in previous devices degraded the energy resolution in the center section of the absorber. With a different contact configuration, we have eliminated this spatial broadening. © *2001 American Institute of Physics.* [DOI: 10.1063/1.1391422]

Detectors based on superconducting tunnel junctions (STJs) have been studied in the last decade as nondispersive single-photon spectrometers for photon energies of 1 eV–10 keV.[1–6] The small superconducting energy gap, ~meV, compared to the electron-hole excitation energy, ~eV in semiconductors, gives a much larger ($\sim 10^3$) number of excitations. This improves the energy resolution of the STJ detectors compared to semiconductor detectors. STJ-based detectors also provide timing information and high quantum efficiency. The predicted energy resolution has been achieved in the UV and soft x-ray regime,[4] but not yet at photon energies $E>1$ keV.

In a recent letter we proposed a theory of the noise in this higher energy range, $E>1$ keV. The dominant source of the energy broadening is the incomplete cooling of the quasiparticles from the absorbed photon.[7] This incomplete cooling has three main effects: (1) it reduces the junction's dynamic resistance during a pulse, leading to larger current and charge noise, due to the amplifier's voltage noise appearing across a lower resistance; (2) it causes the collected charge to depend much more on the bias voltage, which fluctuates slightly from pulse to pulse since it is an active bias; and (3) it gives less than full collection of the quasiparticle charge as electrons; this leads to partition noise from the quasiparticles which tunnel as holes. Our theory explained the measured energy broadening in the detector studied then, $\Delta E=26$ eV full width at half maximum (FWHM) at $E=5.9$ keV. We predicted that more complete cooling of the quasiparticles would reduce ΔE. We have recently designed a detector using this theory. The design improves the energy resolution to $\Delta E=13$ eV at $E=5.9$ keV. The major improvement of the present work is the reduction of the amplifier–device interaction, largely due to the longer tunnel time of the device.

The devices have a Ta film absorber read out by an Al-based tunnel junction on each end, shown in Fig. 1. This geometry[2,3] provides 1D spatial imaging using the division of the quasiparticle charge between the two junctions. It uses only two readout amplifiers. When a photon with energy E is absorbed into the superconducting Ta film, with energy gap $\Delta_{Ta}=700\,\mu$eV, it breaks Cooper pairs and creates an average number $N_0=E/\varepsilon$ excess quasiparticles [$\varepsilon=1.74\Delta$ (Ref. 1)]. These quasiparticles cool rapidly to the Ta energy gap. They then diffuse until they reach an Al trap electrode on either end of the absorber, where they cool toward the Al gap ($\Delta_{Al}=180\,\mu$eV) by phonon emission, and thus are trapped in the Al once the energy is less than Δ_{Ta}. These quasiparticles then tunnel through the barrier and produce a current pulse that is recorded. This current pulse is integrated to give the charge from each tunnel junction. The ratio of the two charges gives the position of the photon absorption. Their sum gives the photon energy.

The detectors have a Ta absorber about 600 nm thick with area $200\times 100\,\mu m^2$. Table I contains the main parameters for all the devices. Their geometries are shown in Fig. 1. Device B differs from device A in that the junction and trap areas of device B are smaller, and the tunneling time is twice that of device A. Device C has a junction design and, therefore, a predicted energy resolution similar to device A. For devices A[3,6–8] and B[9] we use a higher energy gap material, Nb, as a ground contact. A Nb contact ($\Delta_{Nb}=1.4$ meV) should prevent the diffusion of the quasiparticles out of the lower energy gap Ta absorber. Device C uses a Ta ground contact which connects to one of the Al traps.

The measurements are conducted in a two-stage pumped ^{3}He cryostat at 210 mK. A magnetic field of about 2.5 mT is applied parallel to the substrate, to suppress the Josephson current. The devices are irradiated with an ^{55}Fe x-ray source which emits Mn $K_{\alpha 1}$ (5899 eV), Mn $K_{\alpha 2}$ (5888 eV), and Mn K_β (6490 eV) lines with an intensity ratio of 100 : 51 : 18 with a natural linewidth about 2.8 eV. The calculated absorption efficiency at 5.9 keV is 28%. A low noise current amplifier is used to measure the current signal from each

a)Electronic mail: daniel.prober@yale.edu

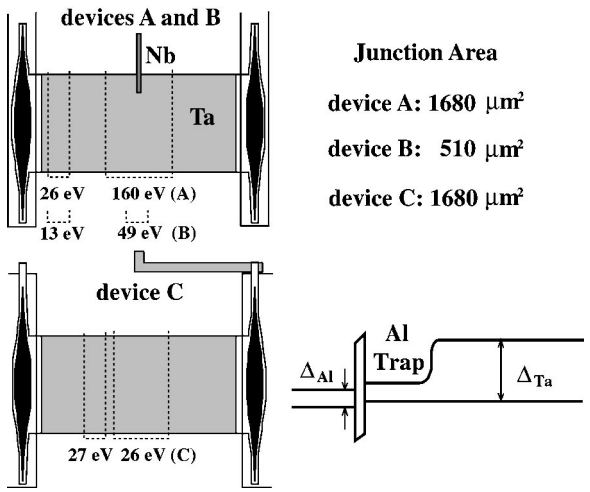

FIG. 1. Geometry of devices A, B, and C. Total energy width ΔE_{total} is shown for the specified region of each device. The black regions are the tunnel junctions. The Ta absorber is 200 μm long. A band diagram of one of the two junctions is also shown.

tunnel junction.[8] For device A, the feedback resistor of the amplifier is at room temperature. For the other two devices the feedback resistor is at 1.5 K, so that its Johnson current noise is negligible. The energy width due to amplifier current noise (input noise and feedback resistor) is measured by injecting electronic pulses through the junctions in the quiescent state (i.e., without x rays).

The energy broadening (FWHM) due to device noise alone (i.e., with a perfect amplifier) is given by $\Delta E_{\text{device}} = 2.355\ (\varepsilon E F_{\text{eff}})^{1/2}$. F_{eff} includes terms that account for the correlation in the creation statistics of the quasiparticles,[10–12] for the tunneling statistics,[13,14] for incomplete charge collection at low voltage bias,[7,15] for quasiparticle losses in the absorber, for multiplication of quasiparticles when they are trapped from Ta into Al, and for self-recombination of the quasiparticles in the Al trap. With the inclusion of all these effects, F_{eff} can be energy-dependent. The best resolution that can be achieved is that limited by just the creation statistics. For this, $F_{\text{eff}}=0.22$, and for absorption of 5.9 keV photons in Ta, the energy broadening is $\Delta E_{\text{creation}}=2.9$ eV. STJ devices studied to date at 6 keV do not achieve this value of ΔE. The predicted values of ΔE_{device} are given in Table II. Devices B and C have somewhat reduced ΔE_{device} because many fewer quasiparticles are lost from their Ta absorbers.[18] Device B has a longer tunnel time and larger allowable bias voltage (see below), and thus achieves more complete charge collection. This reduces the device energy width. However, device B also has broadening due to self-recombination effects resulting from the smaller trap volume. This self-recombination by itself would give a width of 5.3 eV. Use of a larger trap volume can reduce this broadening. Spatial nonuniformity of the absorber response in devices A and B caused additional broadening which we argue below is due to the Nb contact. However, spatial broadening appears to be negligible for device C.

TABLE I. Main parameters of devices studied.

	Device A	Device B	Device C
Junction area (μm^2)	1680	510	1680
R_N (Ω)	0.5	1.4	0.5
Trap volume (μm^3)	700	490	770
Barrier resistance ($\Omega\,\mu$m^2)	840	714	840
Tunnel time (μs)	2.5	4.8	2.5

TABLE II. List of all the noise contributions in devices A, B, and C (FWHM). The source intrinsic linewidth is 2.8 eV.

Energy width-ΔE	Device A ΔE (eV)	Device B ΔE (eV)	Device C ΔE (eV)
Predicted device noise			
Creation	2.9	2.9	2.9
Absorber loss	3.6	$\sim$0	$\sim$0
Trapping multiplication	3.6	3.6	3.6
Backtunneling	5.9	4.8	5.8
Cancellation	4.1	2.5	4.1
Self-recombination	$\sim$0	5.3	$\sim$0
Sum	9.3	8.9	8.5
Amplifier-related noise $\Delta E_{\text{amplifier}}$			
Current noise	11.8	4.2	7.6
Voltage noise	16.8	5.3	16.8
Bias-voltage fluctuations	10.6	3.5	10.6
Sum	23.1	7.6	21.3
ΔE_{total} predicted	25.0	12.0	23.1
ΔE_{total} measured	25.4 ± 2.1	13.1 ± 1.6[a]	26.0 ± 2.1

[a]This width has been corrected for the slight nonlinearity of the junction response due to self-recombination.

The energy width $\Delta E_{\text{amplifier}}$ has three main contributions, as listed in Table II. These are due to (1) amplifier ''current noise;'' (2) the amplifier voltage noise applied across the device resistance, in the signal bandwidth (listed in Table II as ''voltage noise''), which is larger if the differential resistance of the device during the pulse is small, and (3) low-frequency amplifier noise (<100 Hz) which varies the gain of the detector from one photon to the next (listed as ''bias fluctuations'') since the collected charge depends on bias voltage. The current noise for device A has significant contributions from the room temperature feedback resistor, mechanism (1). All three mechanisms contribute to $\Delta E_{\text{amplifier}}$, adding in quadrature. Finally, the x-ray source has finite linewidth, $\Delta E_{\text{source}}=2.8$ eV. Adding all these contributions, we predict in Table II the total energy width: $\Delta E^2_{\text{total}}=\Delta E^2_{\text{device}}+\Delta E^2_{\text{amplifier}}+\Delta E^2_{\text{source}}$, and we list the measured total width, which is smallest for device B.

In a previous letter[7] we showed that the nonequilibrium distribution of the excess quasiparticles in the trap of device A caused the large contributions from ''voltage noise'' and bias fluctuations. Device B has a longer tunnel time, and thus the quasiparticles cool longer. The device thus has a larger differential resistance during the current pulse. This significantly reduces broadening due to amplifier voltage noise and bias fluctuations. The smaller junction dimension of device B also causes its Fiske modes to occur at higher voltage than for devices A and C, allowing use of a larger bias voltage, $V=120\,\mu$V. This further reduces the contributions to $\Delta E_{\text{amplifier}}$. These differences are evident in Table II. The predicted amplifier noise of device C is like that of device A,

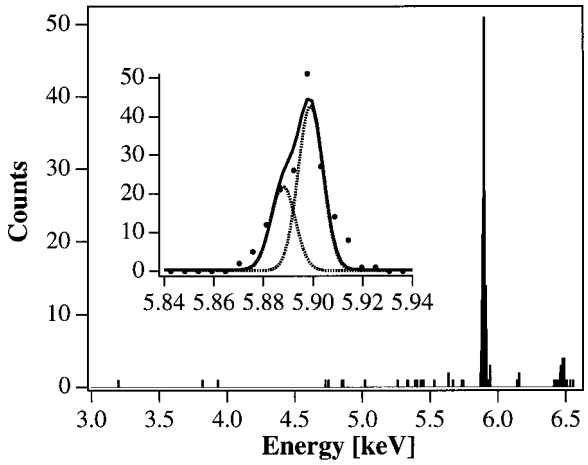

FIG. 2. Energy spectrum over a $20\times100\,\mu m^2$ range of Ta absorber of the device B illuminated with a ^{55}Fe source. The inset shows the Mn $K_{\alpha1}$ and Mn $K_{\alpha2}$ lines with their fits of $\Delta E=13$ eV to theory.

except that we use a cold feedback resistor with device C, for reduced current noise.

An x-ray spectrum obtained from device B is shown in Fig. 2. The theoretical fit uses the $K_{\alpha1}$ and $K_{\alpha2}$ lines with their known intensity ratio. Device B achieves its best energy resolution of ΔE_{total} (FWHM) $=13.1\pm1.6$ eV in a selected region with area of $20\times100\,\mu m^2$ near the side of the absorber.[16] Device A achieves $\Delta E_{\text{total}}=26$ eV in a similar region of the absorber. Device B shows some nonlinearity due to self-recombination of the excess quasiparticles before they tunnel.[17] The total energy resolution we calculate from the theory is consistent with the experimental results for all three devices.

We see in Fig. 1 that the energy width of devices A and B is not uniform along the absorber. It is worst in the middle.[18] The fact that the energy width is large in the middle of devices A and B suggests that the broadening may be related to the Nb contact. A niobium contact was used because its larger energy gap should prevent diffusion of quasiparticles out of the absorber. However, Nb is also known to have metallic oxides, which may form local trapping sites where the Nb contacts the absorber. If trap states exist at or near the Nb–Ta interface, quasiparticles that are produced relatively far from the Nb contact can diffuse there and be trapped and lost, reducing the collected charge. The Nb strip only contacts one side of the absorber. This loss would vary in magnitude for photons absorbed at different positions along the midline of the absorber, being largest for absorption events near the Nb contact. This would produce a large spatial nonuniformity of the detector response, degrading the energy resolution.

We tried to improve the uniformity by replacing the Nb ground contact to the absorber with a Ta contact to one of the Al traps, in device C. With the Ta contact the energy resolution is not degraded in the center. In fact, we achieve an energy resolution of 26 eV in a large region in the center, of area $50\times100\,\mu m^2$. The average energy resolution for the whole active region of the absorber in device C is 32 eV. This experiment with device C confirms that the Nb contact caused the degraded energy resolution in the middle of the devices A and B. The improved uniformity and resolution will be important for realizing a practical imaging detector. With junctions like those of device B and with a Ta contact to the Al trap, an energy width $\Delta E_{\text{total}}=13$ eV should be achieved over the whole device. We will fabricate such a device in the future. According to our theoretical treatment, further improvements are possible by using a larger trap and a different junction shape to allow biasing at higher voltage.

The authors thank K. Segall, M. Devoret, S. Friedrich, and R. Schoelkopf for useful discussions. Research was supported by NASA and NASA-GSFC.

[1] N. Booth and D. J. Goldie, Supercond. Sci. Technol. **9**, 493 (1996).
[2] H. Krauss, F. v. Feilitzsch, J. Jochum, R. L. Mossbauer, T. Peterreins, and F. Probst, Phys. Lett. B **321**, 195 (1989); J. Jochum, H. Krauss, M. Gutsche, B. Kemmather, F. v. Feilitzsch, and R. L. Mossbauer, Ann. Phys. **2**, 611 (1993).
[3] S. Friedrich, K. Segall, M. C. Gaidis, C. M. Wilson, D. E. Prober, A. E. Szymkowiak, and S. H. Moseley, Appl. Phys. Lett. **71**, 3901 (1997).
[4] P. Verhoeve, N. Rando, A. Peacock, A. van Dordrecht, B. G. Taylor, and D. J. Goldie, Appl. Phys. Lett. **72**, 3359 (1998); J. B. le Grand, C. A. Mears, L. J. Hiller, M. Frank, S. E. Labov, H. Netel, D. Chow, S. Friedrich, M. A. Lideman, and A. T. Barfknecht, *ibid.* **73**, 1295 (1998).
[5] P. Hettl, G. Angloher, F. v. Feilitzsch, J. Hohne, J. Jochum, H. Kraus, and R. L. Mossbauer, Proceedings of EDXRF'98, Bologna, 7–12 June 1998; G. Angloher, B. Beckhoff, M. Buhler, F. v. Feilitzsch, T. Hertrich, P. Hettl, J. Hohne, M. Huber, J. Jochum, R. L. Mossbauer, J. Schnagl, F. Scholze, and G. Ulm, Nucl. Instrum. Methods Phys. Res. A **444**, 214 (2000).
[6] K. Segall, C. M. Wilson, L. Li, A. K. Davies, R. Lathrop, M. C. Gaidis, D. E. Prober, A. E. Szymkowiak, and S. H. Moseley, IEEE Trans. Appl. Supercond. **9**, 3226 (1999).
[7] K. Segall, C. M. Wilson, L. Frunzio, L. Li, S. Friedrich, M. C. Gaidis, D. E. Prober, A. E. Szymkowiak, and S. H. Moseley, Appl. Phys. Lett. **76**, 3998 (2000).
[8] S. Friedrich, K. Segall, M. C. Gaidis, C. M. Wilson, D. E. Prober, P. J. Kindlmann, A. E. Szymkowiak, and S. H. Moseley, IEEE Trans. Appl. Supercond. **7**, 3383 (1997).
[9] L. Li, L. Frunzio, C. M. Wilson, K. Segall, D. E. Prober, A. E. Szymkowiak, and S. H. Moseley, IEEE Trans. Appl. Supercond. **11**, 685 (2001).
[10] K. Segall and D. E. Prober (unpublished).
[11] For Sn: M. Kurakado, Nucl. Instrum. Methods **196**, 275 (1982); for Nb: N. Rando, A. Peacock, A. van Dordrecht, C. L. Foden, R. Engelhardrt, B. G. Taylor, J. Lumley, and C. Pereira, Nucl. Instrum. Methods Phys. Res. A **313**, 173 (1992). We assume Ta to be similar to these two metals.
[12] U. Fano, Phys. Rev. **72**, 26 (1947).
[13] D. J. Goldie, P. L. Brink, C. Patel, N. E. Booth, and G. L. Salmon, Appl. Phys. Lett. **64**, 3169 (1994).
[14] C. A. Mears, S. E. Labov, and A. T. Barfknecht, Appl. Phys. Lett. **63**, 2961 (1993).
[15] K. Segall, Ph.D. thesis, Yale University, 1999.
[16] The uncertainties listed for ΔE_{total} in Table II are extracted from our data analysis. We produce a histogram of the charge of the recorded current pulses according to the charge collected, after digital filtering of the integrated current waveform. We use a specific ''bin'' size for the charge unit. To ensure that our choice of bin size does not distort our determination of ΔE_{total}, we repeat the histogram analysis for ten different choices of bin size. The reported rms variation of 1.6 eV for device B, for example, characterizes the variation for different bin sizes of the values determined for ΔE_{total}.
[17] The ratio of the charge collected in the Mn K_β line to the one in the Mn K_α line is 1.09 instead of 1.10. The corrected experimental energy resolution of 13 eV has been obtained after considering the nonlinear response.
[18] The Nb film of device A was of lower quality than device C.